RSC Advances

ROYAL SOCIETY OF CHEMISTRY

www.rsc.org/advances

Journal Name

ARTICLE

Following nanoparticles in complex turbid media

A. Mikhailovskaya,[a] J. Crassous,[b] A. Salonen,[a] and D. Langevin[a]

Received 00th January 20xx,
Accepted 00th January 20xx

DOI: 10.1039/x0xx00000x

www.rsc.org/

Diffusing wave spectroscopy (DWS) was used to determine the size and volume fraction of nanoparticles (NP) within a foam taken as an example of a turbid media. The presence of two types of scatterers - dispersed NPs and liquid/gas interfaces - leads to a two-fold dynamics in the system. Two characteristic decays of the temporal autocorrelation function are observed, their position and amplitude are dependent on particle concentration and foam age. Since only those NPs which are performing Brownian motion decorrelate the signal, one can follow the dynamics of particles' trapping into the foam matrix during the evolution of the system. The technique is a direct and noninvasive way to detect NPs in turbid media. The detection limit strongly depends on the NP nature and the algorithm for its estimation is provided.

Introduction

The importance of disperse systems in our daily lives is enormous. They compose a range of products and materials in food, cosmetics, medicines and health-care products, where particle dispersions, gels, emulsions, foams and often their combinations are found. While disperse systems are commonly used and widely spread, their metastability and finite lifetime pose problems during usage in many of the applications. The structural evolution during the aging eventually results in the complete destruction of the system[1]. The necessity to combine specific properties with stability usually leads to complex formulations and the dispersions often contain surfactant micelles, particles and their aggregates, oil droplets, protein globules etc[2]. Interactions are possible both between these components and the matrix and between the components themselves. This fact together with the turbidity of the dispersions makes it difficult to follow the internal dynamical processes which control the system lifetime.

An additional difficulty in the case of foam is that their study requires the application of non-invasive methods: treatments such as dilution, drying, freezing etc. result in sample damage. The non-invasive method of diffusing wave spectroscopy (DWS)[3,4] has therefore be widely used for the characterization of foam evolution. With this method, the frequency spectrum of the transmitted or reflected light can be related to the multiple scattering events of photons. Information about structural rearrangements can be obtained[5,6]. Instead of the light spectrum, and as in classical dynamic light scattering (DLS)[7,8], the correlation function of the scattered light is generally measured, this function being the Fourier transform of the light power spectrum. Recently DWS was also applied to more complex dispersions containing colloidal particles dispersed in a foam[9,10], where the system evolution was determined both by Brownian motion of the freely diffusing colloids and by aging of the foam. Taking this foam mixed with nanoparticles as a model system, it was shown that the interpretation of the results can be considerably biased because of the traces of dispersed colloids[9]. This can be particular important in food science since DWS is a traditional tool for food microrheology[11] and it is commonly used to follow the dynamics of gelling systems[12].

The corresponding theoretical model was proposed in [9], however the limits of application of the method remained open for discussion. We used a specially designed measuring cell which allowed to carry out the experiments for different thicknesses but in the same foam and at the same age of the sample. This method allows to prove the validity of the model and to determine the range of applicability of this DWS method. We studied a Gillette shaving foam with two different types of nanoparticles, silica and latex.

Another motivating question was the feasibility of the measurement of particle concentration in turbid media. This is not a trivial problem for the light scattering methods, although the use of DLS[13] and diffused photon density wave spectroscopy (DPDWS)[14] are reported in the literature. However DLS requires considerable dilution of the sample, which is complicated with delicate samples. The use of DPDWS is not very common although it has been used to measure micellar aggregation in a turbid solution. In the present work, we have studied in detail the issue of measuring the particle concentration within the evolving matrix.

The article is structured as follows: we start with an introduction to DWS, which finishes with a short summary. The experiments are then described, and we show how the

[a] Laboratoire de physique des solides, UMR 8502 Université Paris-Sud, bât 510, 91405 Orsay cedex
[b]. Institut de Physique de Rennes, UMR 6251, Université de Rennes1,Campus de Beaulieu Bâtiment 11A, 35042 Rennes Cedex
† Footnotes relating to the title and/or authors should appear here.

concentration of nanoparticles can be measured in Gillette foam.

Theory

The concept of diffusing wave spectroscopy (DWS) consists in extending the main principles of photon correlation spectroscopy (generally known as dynamic light scattering - DLS) for strongly multiply scattering media[3,4], such as natural and industrial colloidal systems. Similarly to DLS, the sample is illuminated with coherent light, which scatters from the colloids of the suspension, the liquid films of foams or the oil droplets of an emulsion. Disordered rearrangements of these scatterers produce temporal fluctuations of the resulting electric field E and the registered intensity of scattered light I: the difference arises between the signal at the initial moment t and at a later instant $t+\tau$. In other words, the signal decorrelates with delay τ. The rate of these fluctuations is determined by reorganization dynamics of the scattering medium and can be characterized with the following temporal autocorrelation functions

$$\frac{\langle I(t)I(t+\tau)\rangle}{\langle I(t)\rangle^2} \equiv g_I(\tau) = 1+\beta|g_E(\tau)|^2 \equiv 1+\beta\left(\frac{\langle E(t)E^*(t+\tau)\rangle}{\langle |E(t)|^2\rangle}\right)^2 \quad (1)$$

where $g_I(\tau)$ and $g_E(\tau)$ are normalized intensity and field autocorrelation functions. The relation is known as the Siegert relation, and β is a constant determined by the collection optics. The function $g_E(\tau)$ is normalized such that $g_E(\tau=0)=1$, and then $g_I(\tau=0)=1+\beta$. In the case of intensity autocorrelation function for unpolarized scattered light $\simeq 0.5$. If there is a single dynamical process in the system both autocorrelation functions steeply decay at a characteristic value of τ related to the rate of reorganization of the scatterers (in both transmission or backscattering). Thus information on internal dynamical processes can be obtained in the following way.

A photon traveling through highly scattering media undergoes many scattering events and changes its initial direction of propagation. Once the photons have travelled over the distance l^*, the transport mean free path, the direction is assumed to be totally randomized and light propagation can be modeled with a diffusion equation[3]. Thus the photons arriving to the detector have taken random paths of various lengths. The paths are distinct from each other with a different number of scattering events and, consequently, they create different phase variations. We note $\Delta\varphi_s(t,t+\tau)$ the phase difference for a path of length s between times t and $t+\tau$. Temporal fluctuations reflect normalized path distribution

$$\boldsymbol{P(s)} = \int_{\boldsymbol{s}} \boldsymbol{P(s)ds} = \mathbf{1}.$$

The autocorrelation function can be expressed as

$$g_E(\tau) = \int P(s) g_E^{(s)}(\tau) ds \quad (2)$$

where $g_E^{(s)}$ is the field autocorrelation function for a path of length s directly depending on the acquired phase shift $\langle e^{-i\Delta\varphi_s(t,t+\tau)}\rangle$ and $P(s)$ is calculated in the frame of the diffusion approximation[3,15].

If light is scattered by a dispersion of particles, their Brownian motion causes temporal fluctuations of intensity and the rate of signal decorrelation is related to particle size: the autocorrelation function decays faster in the case of smaller particles[3]. The character of scattering in foams is different. Light is scattered by the liquid/gas interfaces and the decorrelation of the signal arises from the reorganization of the foam skeleton during the evolution of the system[16]. The characteristic time between structural rearrangement events determines the position of the autocorrelation function decay.

In the case of a mixture of foam and NPs, the presence of two kinds of scatterers results in a twofold dynamics in the system. The solution of the problem has been demonstrated in detail elsewhere[9], and considers the impact of both dynamical processes in the decorrelation rate. The characteristic timescale of bubble reorganization is taken as $\tau_R = 1/Al^*$, where A is a constant depending on the bulk properties of the dispersion and l^* is of the order of a few bubble diameters. For the Brownian motion of NPs in the continuous liquid phase the characteristic time is $\tau_B = 1/4k^2D$, where D is the Brownian diffusion coefficient of colloidal particles, $k = 2\pi n/\lambda$, with λ the wavelength inside the material and n the refractive index of the continuous media. The contribution of colloidal particles to the total scattering can be characterized by introducing the mean distance l_C between two scattering events by NPs. The definition is related to the number of NPs in a sample, $l_C = 1/n_C\sigma_C$, where n_C is the number of particles per unit volume and σ_C is the scattering cross-section of the particles. Considering the probabilities of indicated scattering events, it has been shown[9] that the field autocorrelation function in the case of a parallel slab of thickness L is

$$g_E(\tau) \cong \exp\left[-\frac{L^2\tau}{2(l^*)^2\tau_R} - \frac{L^2}{2l^*l_C}\left(1-g_E^{(B)}(\tau)\right)\right] \quad (3)$$

where

$$g_E^{(B)} = \frac{1-\exp\left(-\tau/\tau_B\right)}{\tau/\tau_B} \quad (4)$$

is the correlation function for single scattering from Brownian NPs taken as a point like scatterers.

To summarize briefly, the dynamical processes in the system cause temporal fluctuations of the signal – the intensity of scattered light. The rate of these fluctuations is characterized by the autocorrelation function. This function describes the extent of correlation (or simply similarity) between signals separated by a certain time segment. The decay of the function depends on the rate of the corresponding internal dynamics of the system, i.e. on the size and number of scatterers.

Materials and methods

Commercial shaving foam Gillette Regular was chosen as a model system. This kind of foam is often used to investigate the physics of foams – optics[17], acoustics[18] and rheology[19] –

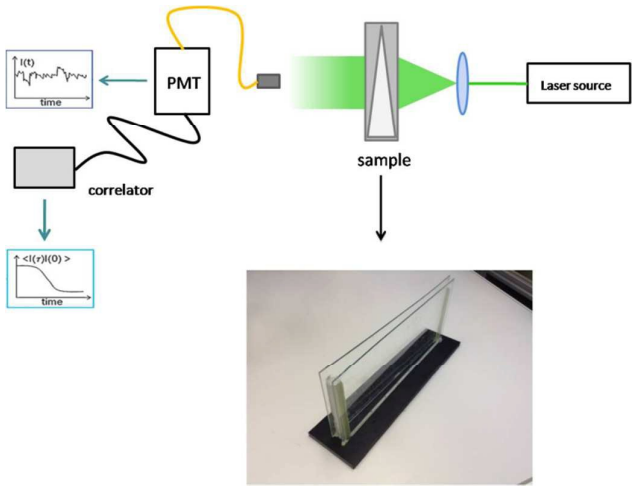

Fig. 1. Scheme of the experimental setup.

because of its excellent stability and almost complete absence of drainage and coalescence during up to 3 days[16]. Physical properties of Gillette Regular are quite reproducible and well established. It is reported that the initial liquid fraction is ≃ 8%[5], viscosity of the continuous phase is 1.9 cP[20] and the refractive index of the liquid phase $n = 1.344$, close to the value for water. We used two kinds of nanoparticles with different affinities to the solvent of the foam continuous phase (water), latex beads and silica particles. The surface of latex beads LB-1 (Sigma-Aldrich) contains hydrophobic polystyrene groups and the stock aqueous dispersion is stabilized against flocculation with a small amount of surfactant. The beads are monodisperse with a mean diameter of 100 nm. An LB-1 dispersion with a solid volume fraction of 10% was used as received. More hydrophilic silica NPs were used. The aqueous sodium-stabilized dispersion Levasil 30/50 (AkzoNobel) contains 50% solid volume fraction. The size of the particles was determined in a 100 ppm aqueous solution using a nanosizer Delsa Nano C. The size distribution is monomodal with a peak at a diameter of 130 nm.

To prepare a sample with a specific volume fraction of NPs Φ_C, defined as the volume of colloidal particles over the volume of the foam, we followed the procedure described in ref. 9. A controlled volume of NP suspension was added to a fixed mass of foam and the mixture was stirred for 1-2 minutes.

Afterwards the mixture was placed in the measuring cell, the glass walls of which are at an angle of about 2° (Fig. 1). This geometry makes it possible to carry out measurements for various thicknesses in the same foam at similar ages without preparing numerous samples for the same system. The length of the cell is 28 cm and the height of the walls is 10 cm. With this cell one can vary the sample thickness roughly between 5-10 mm while avoiding any leakage of scattered light and being sure that the measurements are made in the multiple scattering regime ($L \gg l^*$).

The scheme of the experimental setup is presented in Fig.1. The measurements were carried out in the transmission configuration. Since the method is based on the measurement of the averaged intensity of the scattered light, the probing area was extended by expanding the laser beam (532 nm, 100 mV, Compass 315M from COHERENT) with a lens. The resulting diameter of the light spot was around 5 mm. Doing this one can be sure that even for aged foams, with bubbles of diameter up to about 200 μm[16], the signal is averaged over sufficient numbers of bubbles. The intensity of scattered light was measured with a single-mode optical fiber with collimation optics. The fiber output is sent to a photomultiplier, and the normalized intensity autocorrelation function $g_I(\tau)$ is measured with a digital correlator (Flex03LQ-12 from Correlator.com) operating in multi-tau mode. The typical photon rate is 7-10 kHz and correlation functions are obtained after 1-5 min averages depending on signal statistics.

Experimental results

The samples under investigation contain two types of scatterers (Fig. 2). The first ones are NPs dispersed in a continuous medium and subject to Brownian motion. The second ones are the foam Plateau borders, which undergo reorganization because of changes in bubble neighbours during the foam evolution. The rate of the first process relates to the size of particles, which is about 100 nm in our case. The scale of foam structural rearrangements is of the order of 10 bubble diameters[5], which changes from 20 to 200 μm in 1000 min[16] due to coarsening. Thus the temporal fluctuation of the light intensity is caused by dynamics with different rates – "fast" movement of small NPs and "slow" foam structure reorganization. Two decays can be present in the autocorrelation curves. The "fast" decay in the region of a microsecond corresponds to the decorrelation due to the presence of small colloidal particles. The timescale of this decay should stay constant provided the size of scatterers (and consequently the diffusion coefficient) doesn't change during the experiment. In other words, if the nanoparticles don't form clusters, τ_B will remain constant. In contrast, since the radius of bubbles increases during aging due to coarsening, the

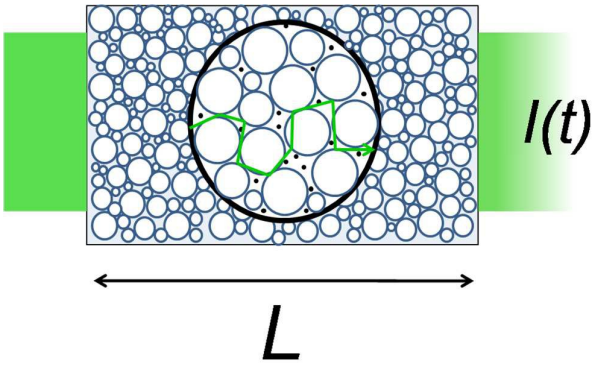

Fig. 2. The slab geometry of the DWS experiment: L is the thickness of the sample, I(t) is the transmitted intensity of the scattered light. In the black circle: zoom showing in green the path of one photon through the system under investigation, foam with particles dispersed in the continuous medium.

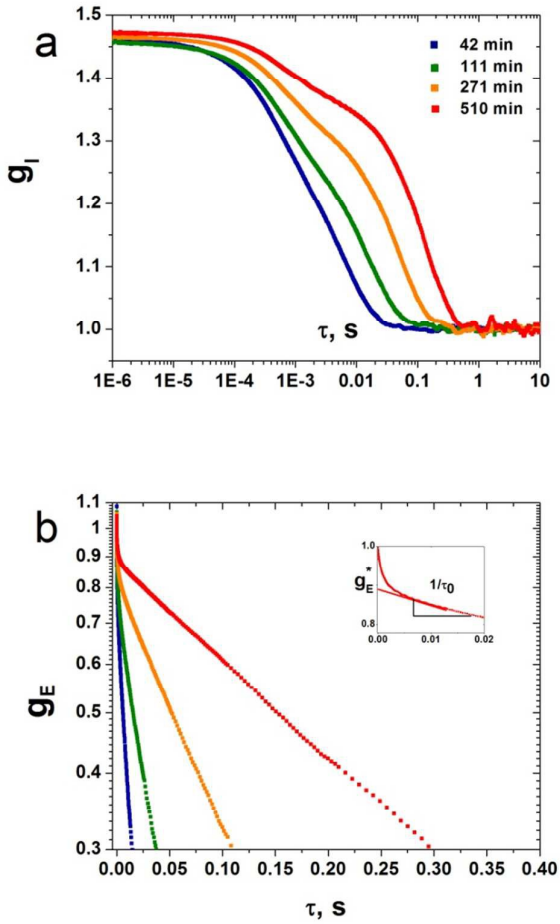

Fig. 3. Autocorrelation functions (a) $g_I(\tau)$ and (b) $g_E(\tau)$ for the mixture of Gillette foam with silica NP ($\Phi_C = 1.3 \cdot 10^{-4}$) at various system ages at the sample thickness of $L = 8.5\ mm$. The inset illustrates the definition of g_E^* and τ_0.

scattering characteristics are changed. The reorganization time τ_R increases from a few microseconds in the beginning of the experiment to ~ 1 s after 1000 min of foam age[5]. In Fig. 3 (a) and (b), the autocorrelation functions $g_I(\tau)$ and $g_E(\tau)$ for the mixture of Gillette foam with silica NPs at different ages are presented. These functions describe the same process but they have distinct normalizations and are presented here in different coordinates. One can see in Fig. 3 (a) that $g_I(\tau)$ decreases between two plateaus. After the higher plateau at small τ, one still sees a correlation in the signals.

The lower plateau at long times corresponds to a complete loss of correlation. The decay rates τ_B and τ_R correspond to the two dynamical processes. At an early age of the system, τ_B and τ_R are quite close to each other and the decays are merged and indistinguishable. Upon foam aging, the bubble size increases, τ_R shifts towards longer times and is about 0.2 s eight hours after sample preparation. Then the two decays related to the different dynamical processes become well separated and an intermediate plateau appears. The same tendency is observed in Fig. 3 (b) for the normalized $g_E(\tau)$ In a log-lin scale: one can distinguish between the slopes of the "fast" decay due to the Brownian motion of particles and the "slow" decay related to bubble rearrangements, which is getting more pronounced.

In ref.9 it is shown that the intercept of the exponential decay of $g_E(\tau)$ (and consequently the height of the intermediate plateau of $g_I(\tau)$ after the fast decay) depends directly on the volume fraction of colloidal particles. In the limit $\tau \gg \tau_B$, $g_E^{(B)} \cong 0$ and the electric field autocorrelation function (3) can be written as

$$\ln(g_E(\tau)) = \ln(g_E^*) - \tau/\tau_0 \quad (5)$$

where $g_E^* = \exp(-L^2/2l^*l_C)$ and $\tau_0 = 2(l^*)^2\tau_R/L^2$. The value of g_E^* depends on l_C, and thus on the concentration of NPs in the system. It has been shown[9], that for a fixed age and thickness of the sample an increase of the nanoparticle volume fraction results in lowering of the value of g_E^*, e.g. the first fast decay becomes more pronounced and less correlations remain

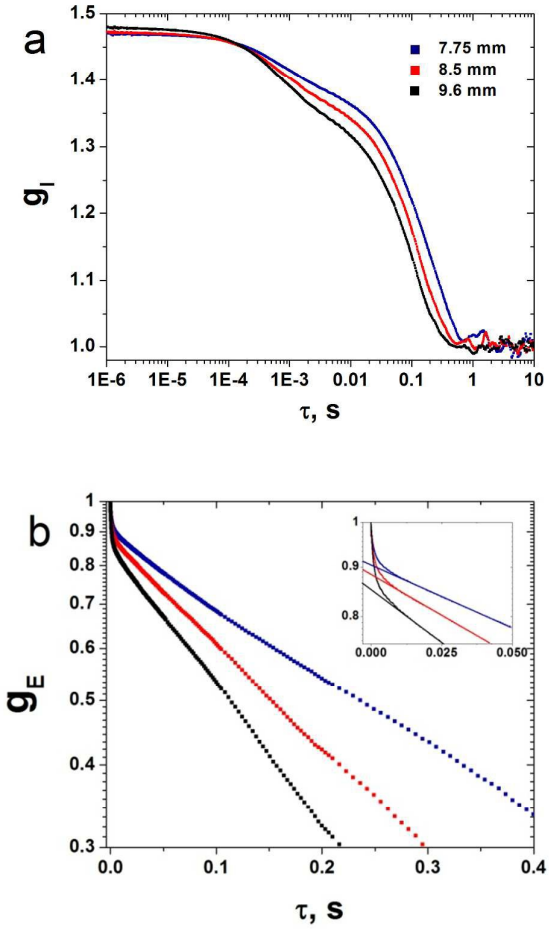

Fig. 4. Autocorrelation functions (a) $g_I(\tau)$ and (b) $g_E(\tau)$ (zoomed in the inset) for the mixture of Gillette foam with silica NP ($\Phi_C = 1.3 \cdot 10^{-4}$) at various cell thickness and at the same sample age.

in the system. The decorrelation corresponding to the presence of NPs might also be enhanced by increasing the number of scatterers on the laser beam way. For this purpose, one can increase the cell thickness L. This is illustrated in Fig. 4 (a) and (b), where the curves of the autocorrelation functions $g_I(\tau)$ and $g_{\mathrm{E}}(\tau)$ for the same samples (fixed NP volume fraction and similar age) but with various cell thicknesses are presented. We see that the variations in sample thickness do not influence the fast decay time τ_B. However, the amplitude of the fast decay of $g_{\mathrm{E}}(\tau)$ varies with the cell thickness (see inset of Fig. 4 (b)). This is in agreement with $g_E^* = \exp(-L^2/2l^*l_C)$: for a given sample, the value of g_E^* decreases with L and the thicker the sample, the steeper the drop. The slow decay time of the correlation function depends on the cell thickness in agreement with $\tau_0 = 2(l^*)^2\tau_R/L^2$.

The dependencies of the correlation functions $g_E(\tau)$ with the geometry of the cell L and with the properties of the material may be separated by rewriting (3) as

$$\ln(g_E)/L^2 \cong -\frac{\tau}{2(l^*)^2\tau_R} - \frac{1-g_E^{(B)}}{2l^*l_C}$$

where the last term depends only on material properties. To check this scaling, we carried out measurements for the same foam mixtures with silica NP at the age of more than 1 day (Fig. 5 (a)).

Since the duration of the experiment was a few minutes, we can be sure that the system didn't evolve significantly and that the scattering properties didn't change dramatically during the measurements. The cell we use allows us to vary the sample thickness in the range of 5-10 mm. Due to the cell filling method, air cavities within the sample are sometimes present. This makes it difficult to carry out measurements properly over the full range of cell thicknesses on the same sample. Nevertheless, in Fig. 5 (a) one can see that the coincidence of the curves is good within experimental error. Furthermore the experiments were repeated using latex nanobeads as NPs (Fig. 5 (b)). In this case the scaling of data is also observed.

Thus it is shown that the developed theory adequately describes dynamics in the system and can be used to monitor its evolution.

Determination of NP volume fraction

The main goal of our investigation is to measure the volume fraction of NP in complex media. As we mentioned above, this information can be retrieved from the value of g_E^*, which can be found by fitting the exponential decay with eq. (5) in the range of relatively long times (see the inset of Fig. 3(b) as an illustration). From $g_E^* = \exp(-L^2/2l^*l_C)$ and $l_C = {}^1/_{n_C\sigma_C}$, the number of NP per unit volume can be expressed as

$$n_C = -\frac{2l^* ln g_E^*}{L^2\sigma_C}$$

We assume that the values of the scattering cross-section σ_C of the spherical colloidal particles dispersed in the foam can be calculated with Mie theory[21]. The refractive index of particles is 1.46 and 1.60 for silica and latex respectively, the refractive index of the medium surrounding the particles is 1.344. This assumption may be tested with a complementary experiment where we performed measurements on the same system (same cell thicknesses, same foam age, same NPs and their concentrations), with two different optical wavelengths. Data are plotted in fig. 6. We see that the slow decays are the same, but that the values of g_E^* are different. The values of n_C and L are independent of the wavelength, and we expect the values of l^* to be very close at the two wavelengths. Indeed scattering in foam is mainly due to reflection and refraction which depends on liquid refractive indices, which do not appreciably depend on wavelength. This is supported by the fact that the slow time decays are the same for the two samples.

We then expect the ratio $(lng_E^*)/\sigma_C$ to be independent of the optical wavelength. We found for our systems that the values of lng_E^* vary by a factor of two, but the values of $(lng_E^*)/\sigma_C$ vary by less than 10% ($(lng_E^*)/\sigma_C = 5.1\cdot10^{-3}nm$ at 532nm, $(lng_E^*)/\sigma_C = 4.7\cdot10^{-3}nm$ at 633 nm). This analysis supports

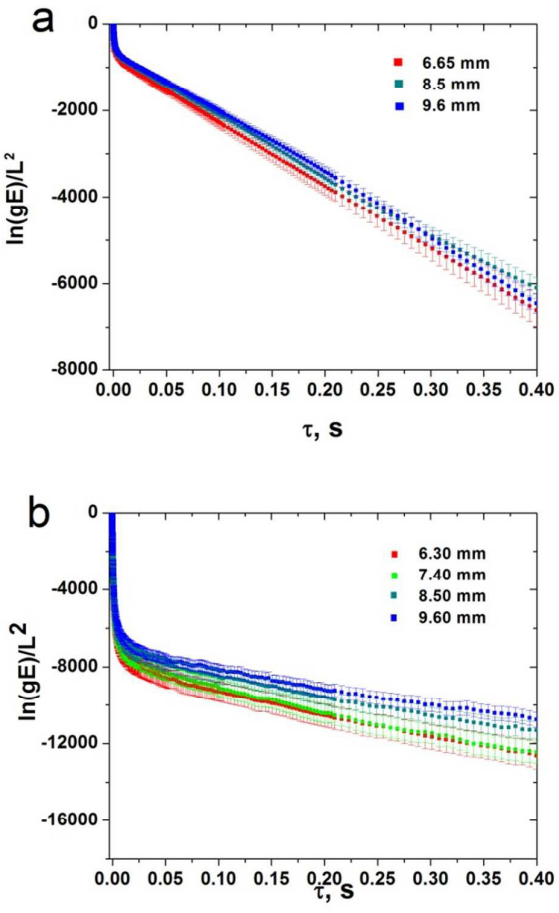

Fig. 5. Master curves for a mixture of Gillette foam with (a) silica NP ($\Phi_C = 1.3\cdot10^{-4}$) aged 24 hours and (b) latex beads ($\Phi_C = 1.4\cdot10^{-4}$) aged 27 hours.

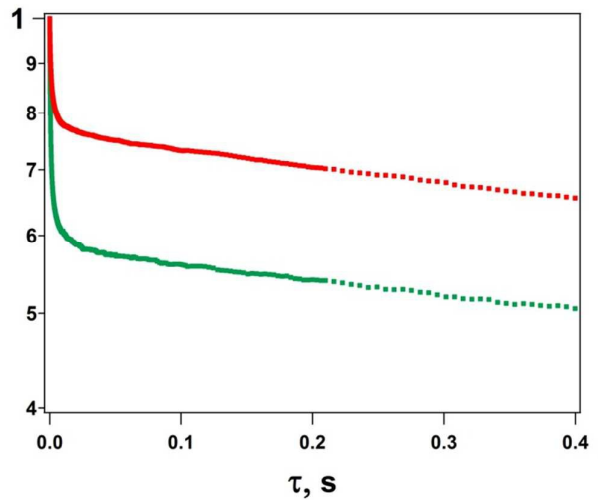

Fig. 6. Normalized autocorrelation functions for a Gillette foam with volume fraction of silica NP $1.47 \cdot 10^{-3}$ measured at laser wavelengths 633 nm (red squares) and 532 nm (green squares).

the fact that Mie scattering may be used to estimate the scattering cross section of a NP in the liquid phase. At the laser wavelength of 532 nm, we calculated for silica NP $\sigma_C = 112\ nm^2$ and for latex nanobeads $\sigma_C = 108\ nm^2$.

The values of l^*may be measured by numerous techniques. However as Gilette foam has been used in many DWS studies, we use here the empirical formulas for the values of $l^{*2} = l_0^{*2} + at_w$ with $t_w$the age of the foam, and l_0^* and a two numerical constants[22]. The added NP should not modify noticeably the value of l^* of the material.

We can now calculate the volume fraction of NPs for our two samples. For the foam with an input concentration of silica NP $\Phi_C = 1.3 \cdot 10^{-4}$ the volume fraction became $\Phi_C = 9.4 \cdot 10^{-6}$ after 24 hours. In the case of the foam with latex NP (input concentration $\Phi_C = 1.4 \cdot 10^{-4}$) the volume fraction was $\Phi_C = 4.8 \cdot 10^{-5}$ at a foam age of 27 hours. Thus we observed a decrease of NP concentration within the foam during the system aging. Because the estimation of the amount of NPs in the system is made on the basis of the signal decorrelation due to their Brownian motion, the decrease of NP volume fraction means that some of them are immobilized and cannot move randomly anymore. One can also see that the silica NP concentration is decreased more strongly than that of latex NP. To understand the origin of this change we followed the kinetic behaviour of the system.

Time evolution of NP volume fraction

Using g_E^* we have access to the NP concentration only at longer times, when the two decays are clearly separated in time. However, to understand how the NP have disappeared, we measured the concentration since the beginning of the experiment. In order to do this, the correlation function at small lag times can be considered. For this we expand (3) at $\tau \to 0$ and obtain $g_E \cong 1 - \tau/\tau_f$ with

$$(1/\tau_f) = \left(\frac{L^2}{2(l^*)^2\tau_R}\right) + (L^2/4l_C l^*\tau_B).$$

The first time decay is related to the foam dynamics and the second one - to the NP dynamics. For the dilute NP systems the foam dynamics is slower (see Fig. 3) and then $(1/\tau_f) \cong L^2/4l_C l^*\tau_B$. Eventually one can obtain

$$(1 - g_E)l^* \cong Cn_C\tau$$

where $C = L^2\sigma_C/4\tau_B$ is a constant which does not depend on the NP concentration. Such a variation can be used to compare directly two solutions labeled (1) and (2) for the same NP at two different concentrations $n_C^{(1)}$ and $n_C^{(2)}$. The parametric plot $[(1 - g_E)l^*]^{(1)}$ as a function of $[(1 - g_E)l^*]^{(2)}$ is expected to be a straight line crossing at origin and with the slope $n_C^{(1)}/n_C^{(2)}$. Such plots are represented for the two NP solutions at different aging times in Fig. 7 (a) and (b). We observed that the parametric plots are indeed linear at small times and that the slope decreases with the system age. This made it possible

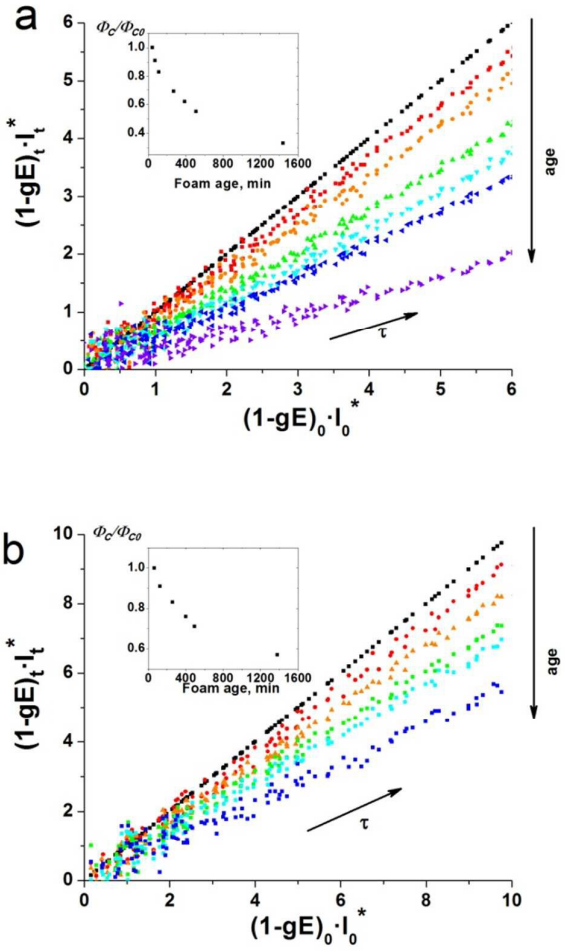

Fig. 7. The ratio between the slopes from (6) demonstrating the decrease of the volume fraction of (a) silica NP and (b) latex beads during the evolution of investigated foam systems. Insets of the graphs represent time evolution of NP volume fraction.

to follow the evolution of the concentration. The observed reduction of NP volume fraction (insets of fig. 7) is related to the decrease of the number of mobile scatterers in the continuous phase. Such a decrease could arise from the aggregation of NPs into larger clusters in the presence of electrolytes and polymers of the Gillette foam. However, the cluster formation would result in an increase of scatterers' size and, consequently, to a shift towards longer times. From the fitting of the $g_E(\tau)$ curves for silica NP we found that $0.45\ ms \leq \tau_B \leq 0.65\ ms$ and for latex beads $0.41\ ms \leq \tau_B \leq 0.57\ ms$, which is in good agreement with the values corresponding to the initial diameter of NPs added to the foam ($0.59\ ms$ and $0.45\ ms$, correspondingly). One can assume that the exclusion of a fraction of NPs from the scattering process occurs because of phenomena leading to the restriction of the NPs Brownian motion in the continuous phase. Taking into account the complex composition of commercial shaving foam one can expect NPs to interact with its components. It seems to be quite possible for NPs to get stuck in clogs formed by polymers or to adsorb on the surface of solid species in the continuous phase or onto bubble surfaces.

Thus the movement of some NPs is blocked and they don't contribute in the fast decay of autocorrelation function.

Application to NP characterization

We have shown that DWS can be used to measure the concentration of NPs in foam. We will now discuss the typical range of concentration that one might access with this method.

Since titanium dioxide (TiO_2) nanoparticles are used for photocatalytic application and as additives for the enhancement of the refractive index in health-care products (sunscreens, some medications, cosmetics), there is a challenge for the detection and characterization of TiO_2 nanoparticles in turbid media[23]. Therefore we will make the calculations by taking NPs of TiO_2 with the diameter of 25 nm as an example.

For simplicity we discuss the experiment in a transmission cell, but the results may be easily extended to other scattering geometries. The basic idea of this method is that the dynamics due to NP is fast compared to the emulsion or foam intrinsic dynamics. The two associated time scales are $\tau_R(l^*)^2/L^2$ for the matrix dynamics, and $\tau_B l_C l^*/L^2$ for the Brownian dynamics. So we expect the two dynamics to be well separated if $(\tau_B/\tau_R) \leq 0.1(l^*/l_C)$. It should be noted that this relation is independent of the cell thickness L and more generally of the scattering geometry. For a typical numerical application, we consider the case of NP of 25nm diameter dispersed in water. The Brownian time is then $\tau_B \cong 0.1\ ms$. If the scattering matrix has an intrinsic reorganization time $\tau_R \cong 1\ s$ and a transport mean free path of $l^* \cong 0.1\ mm$, we should have $l_C \leq 0.1\ m$ for the two dynamics to be well separated. The proper ratio of τ_B/τ_R can be attained by slowing down the dynamics of the matrix, which in the case of a foam simply means to wait until a certain system age.

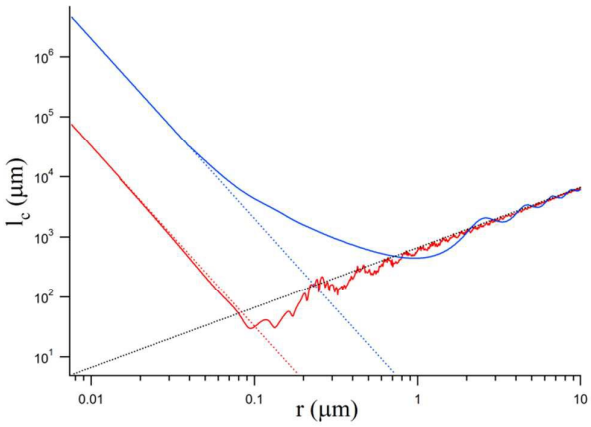

Fig. 8. Values of the scattering lengths as a function of the NP radius. Solutions are at a concentration $\Phi_C = 10^{-3}$. Solid curves are results of Mie scattering for NP: blue - TiO_2, refractive index n=2.67; red - fused quartz, refractive index n=1.46. Optical wavelength is 532 nm, and the surrounding medium is water. Corresponding colored dotted lines are Rayleigh scattering limits, and black dotted line is the limit for large spheres (efficiency factors Q=2)[24].

The value of l_C is related to the concentration of free particles and to their scattering cross section. It may be calculated using Mie scattering theory[21,24]. We plotted in fig. 8 the values of l_C for spherical NP of radius r for a solid concentration of $\Phi_C = 10^{-3}$. For TiO_2 NP of refractive index 2.67 and of diameter 25nm, we find that $l_C \cong 15\ mm$. Since $l_C \propto {\Phi_C}^{-1}$, the condition $l_C \leq 0.1\ m$ becomes $\Phi_C \geq 1.5 \cdot 10^{-4}$. This concentration condition ensures that the two timescales associated with the two dynamics will be well separated.

Coming back to the geometry of the experiment, the cell thickness must be chosen such that the correlation decay due to NP is measurable, but does not mask the decay due to the internal dynamics. The upper limit of NP volume fraction is determined only by the ratio between the sample thickness L and characteristic scattering length scales l^* and l_C and not by the two timescales. Thus if we consider that we may measure accurately $0.1 < g_E^* < 0.99$, we obtain in a transmission geometry a thickness range of $0.07\sqrt{l^* l_C} < L < 1.1\sqrt{l^* l_C}$ (i.e. $0.2\ mm < L < 3.5\ mm$ for the example of TiO_2 NP). The time scale of the decay due to Brownian motion of NP is the same than in the DLS technique and is in the range of usual digital correlators.

We have discussed the possibilities of using the method to study dopant particles, however it could have applications where the particles followed are taking an active part in the dynamics and ageing of the turbid media. Such an example would be particle stabilized foams or emulsions, where the concentrations of adsorbed and free particles could be followed, similarly to that done in [10].

Conclusions

DWS is a powerful technique is sensitive to the movement of nanoparticles and as such can be used for the detection of NPs and for the measurement of their concentration in turbid

media. Through experiments on silica and latex NPs, we illustrated how to measure the concentration of nanoparticles in the system. We also gave the conditions required to be able to measure a NP volume fraction taking nanoparticles of TiO_2 as an example. The method also made it possible to follow the evolution of the system in time, both the medium structure (here coarsening of foam) and the NP dynamics (here Brownian motion). In this way the evolution of the NP concentration can also be monitored and any eventual aggregation followed. In the example studied, the NP volume fraction was found to decrease, not because of aggregation, but because they get trapped at the bubble surfaces due to interactions with the components of the complex medium.

Acknowledgements

We would like to thank Clément Honorez and Jérémie Sanchez for help in the design and construction of the experimental setup. We acknowledge financial support from the European Space Agency and the European Union infrastructure on Nanosafety, QualityNano.

Notes and references

1 D. Weaire and S. Hutzler, *Physics of foams*, Oxford Uni., 2001.

2 E. Rio, W. Drenckhan, A. Salonen and D. Langevin, *Adv. Colloid Interface Sci.*, 2014, **205**, 74–86.

3 D.J.Pine, D. A. Weitz, J. X. Zhu and E. Herbolzheimer, *J. Phys. Fr.*, 1990, **51**, 2101–2127.

4 D. A. Weitz and D.J.Pine, in *Dynamic light scattering: The methods and applications*, Oxford University Press, New York, 1993, p. 652.

5 D. J. Durian, D J, Weitz, D A, Pine, *Phys. Rev. A*, 1991, **44**, 7902–7906.

6 R. Höhler, S. Cohen-Addad and D. J. Durian, *Curr. Opin. Colloid Interface Sci.*, 2014, **19**, 242–252.

7 B. J. Berne and R. Pecora, *Dynamic light scattering with applications to chemistry, biology, and physics*, Dover Publications, 2000.

8 B. Chu, *Laser Light Scattering. Basic Principles and Practice*, Academic Press, 1991.

9 J. Crassous and A. Saint-Jalmes, *Soft Matter*, 2012, **8**, 7683.

10 A. Stocco, J. Crassous, A. Salonen, A. Saint-Jalmes and D. Langevin, *Phys. Chem. Chem. Phys.*, 2011, **13**, 3064–3072.

11 M. Alexander and D. G. Dalgleish, *Fobi*, 2006, **1**, 2–13.

12 M. Alexander and D. G. Dalgleish, *Curr. Opin. Colloid Interface Sci.*, 2007, **12**, 179–186.

13 V. V. Vysotskii, O. Y. Uryupina, a. V. Gusel'nikova and V. I. Roldugin, *Colloid J.*, 2009, **71**, 739–744.

14 J. Tanguchi, H. Murata and Y. Okamura, *Colloids Surf. B. Biointerfaces*, 2010, **76**, 137–44.

15 A. Ishimaru, *Wave Propagation and Scattering in Random Media*, Academic Press, 1978, vol. 8.

16 D. J. Durian, D. A. Weitz and D.J.Pine, *Science (80-.).*, 1991, **252**, 686–688.

17 M. U. Vera, A. Saint-Jalmes and D. J. Durian, *Appl. Opt.*, 2001, **40**, 4210.

18 I. Ben Salem, R. Guillermic, C. Sample, V. Leroy, a. Saint-Jalmes and B. Dollet, *Soft Matter*, 2013, **9**, 1194.

19 A. D. Gopal and D. J. Durian, *Phys. Rev. Lett.*, 2003, **91**, 188303.

20 A. Gopal and D. Durian, *J. Colloid Interface Sci.*, 1999, **213**, 169–178.

21 C. F. Bohen and D. R. Huffman, *Absorption and Scattering of Light by Small Particles*, Wiley VCH, 2004.

22 V. Labiausse, 2004.

23 R. J. B. Peters, G. Van Bemmel, Z. Herrera-Rivera, H. P. F. G. Helsper, H. J. P. Marvin, S. Weigel, P. C. Tromp, A. G. Oomen, A. G. Rietveld and H. Bouwmeester, *J. Agric. Food Chem.*, 2014, **62**, 6285–6293.

24 H. Van de Hulst, *Light Scattering by Small Particles*, Dover Publications, New York, 1981.